Desalination and Water Treatment
www.deswater.com

doi: 10.5004/dwt.2021.27468

231 (2021) 182–195
August

Adsorptive removal of Ni(II) and Co(II) from aqueous solution using succinate-bonded polysaccharide isolated from *Artemisia vulgaris* seed mucilage

Muhammad Ajaz Hussain[a,*], Azhar Abbas[a], Mah Gul Habib[a], Arshad Ali[a], Muhammad Farid-ul-Haq[a], Mazhar Hussain[b], Zahid Shafiq[b], Muhammad Imran Irfan[a]

[a]*Institute of Chemistry, University of Sargodha, Sargodha 40100, Pakistan, Tel. +92 346 8614959; Fax: +92 48 322121; emails: majaz172@yahoo.com (M.A. Hussain), azharabbas73@yahoo.com (A. Abbas), mahgul1818@gmail.com (M.G. Habib), arshadali04@yahoo.com (A. Ali), faridulhaq86@yahoo.com (M. Farid-ul-Haq), imranirfansgd@yahoo.com (M.I. Irfan)*
[b]*Institute of Chemical Sciences, Bahauddin Zakariya University, Multan 60800, Pakistan, emails: hmz14@yahoo.com (M. Hussain), zahidshafiq@bzu.edu.pk (Z. Shafiq)*

Received 31 January 2021; Accepted 28 May 2021

ABSTRACT

Herein, we discuss Ni(II) and Co(II) uptake efficacy of a polysaccharide from *Artemisia vulgaris* (AVH) modified by impregnation with succinic anhydride followed by the treatment with sodium bicarbonate. The ion-exchange affinity of AVH increased significantly after its modification to sodium salt (Na-SAV). The surface charge of sorbent Na-SAV was evaluated by estimating the point of zero-charge pH, that is, pH_{ZPC} and it was found to be 4.75. Sorption data fit well to Langmuir isothermal, pseudo-second-order kinetic and ion-exchange model. Sorption maxima (Q_{max} in mg g^{-1}) of sorbent Na-SAV evaluated from Langmuir isotherm was perceived to be 115.8 mg g^{-1} for Ni(II) and 170.7 mg g^{-1} for Co(II). The values of thermodynamic triplet, such as ΔG°, ΔS°, and ΔH° were appeared negative and revealed exothermic and spontaneous mode of sorption process. Additionally, the sorbent Na-SAV was found regenerated over five repetitive cycles without any prominent decline in sorption capacity.

Keywords: *Artemisia vulgaris* hydrogel; Chemisorption; Ion-exchange; Sorption/desorption; Succinylation

1. Introduction

The reclamation of heavy metals through industrialization, urbanization, technological development, and agricultural activities into the water bodies, lands, and air has become a great concern over the past few decades. The heavy metals, such as nickel (Ni) and cobalt (Co) have many advantages to use in everyday life, that is, Ni(II) is used to prepare corrosion-resistance alloys, and as precursor in lithium-ion batteries [1–3], while Co(II) is essential element of vitamin B12 which in turn necessary for the production of red blood cells [4]. As per recommendations of Word Health Organization (WHO), the threshold level of Ni(II) and Co(II) in drinking water is 0.02 and 0.05 mg L^{-1}, respectively. The release of these heavy metals through natural sources and human activities enhances their limit from permissible and causes severe health risk to living organism. Ni(II) is carcinogenic in nature [5,6] while the discharge of Co(II) damages lungs, kidney, liver, and also causes nausea, cough, asthma, and respiratory problems [7].

Therefore, it is a dire need to eradicate these heavy metals from polluted water and to make it suitable for the utilization of living organisms. Many conventional physical and chemical approaches have been used to get rid

* Corresponding author.

from these toxins [8]. Among those treaties, due to high selectivity and efficiency, ion-exchange method is economically advantageous and is found to be predominantly an attracting scientific attention now-a-days to uptake heavy metal ions from unhygienic water [9,10]. Although biosorbents of natural origin eying the researchers to uptake heavy metal ions from polluted water because of their low costs and environment-friendly nature but all of these have fewer sorption capacities and mostly are not recommended. The efficiency and selectivity of these biomaterials to use them as sorbents can be improve after their chemical modification [11].

A wide array of chemical modifications has been utilized and reported in literature [12]. However, esterification with succinic anhydride found to be more effective and fruitful from many aspects [13]. Furthermore, the presence of natural cross-linking and well-defined functional groups into the backbone of sodic form of these biosorbents make them water insoluble and facilitate to use them in wastewater treatment processes [14]. Among naturally occurring polysaccharides, those present in plant seeds mucilage (PSMs), such as mucilage extruded from *Ocimum basilicum* and *Mimosa pudica* have been reported as excellent materials due to their supersobent nature and reusability. Such polysaccharide materials after chemical modifications, especially succinylation, appeared highly selective for heavy metal ions uptake with regenerable properties [15,16].

Artemisia vulgaris is a plant of mugwort specie. Its seed produced polysaccharide-based thick mucilage, that is, AVH which consists of acetylated sugar. AVH is highly swellable in deionized water and other biological fluids. It offers stimuli-responsive swelling/deswelling (on/off switching) attributes. It is a non-toxic biopolymer and has been utilized as a potent and safe excipient for targeted drug delivery systems. Therefore, due to the presence of sugar moieties in AVH, it is very convenient to introduce carboxylic acid (–COOH) groups on its terminal backbone. These groups can easily be converted to their sodium salts in order to produce an efficient biosorbent for the adsorptive removal of heavy metal ions from contaminated water bodies. AVH is novel biomaterials and have many advantageous features, such as ease of bioavailability, modifiable nature, and reproducibility as compared to other commercially available adsorbent [17,18]. To best of our knowledge, we are the first one to use it as sorbent for the uptake of Ni(II) and Co(II) ions from aqueous solution after its succinylation.

In furtherance of our work, we aimed to extrude and purify mucilage (AVH) from seeds of *A. vulgaris*. The as-isolated mucilage was then tuned with succinic anhydride and sodium bicarbonate in a stepwise manner to prepare its acidic, that is, SAV and sodic, that is, Na-SAV conjugates. Aims are to appraise Na-SAV as efficient and regenerable sorbent for the uptake Ni(II) and Co(II) from aqueous solution. Surface charge on sorbent Na-SAV will be analyzed by point-zero charge (pH_{ZPC}) calculation. The dependence of sorption capacities on different operational parameters such as initial concentration of Ni(II) and Co(II), sorbent dosage, pH, time of contact between sorbent and sorbate and temperature have been exploited. It is also aimed to established sorption mechanism by fitting experimental sorption data to isothermal, kinetics, and ion-exchange models. Thermodynamics of sorption process have been studied by calculating the values of various thermodynamic attributes, such as $\Delta G°$, $\Delta H°$, and $\Delta S°$.

2. Experimental

2.1. Reagent and materials

Seeds of *A. vulgaris* were acquired from Seed Needs, LLC., and used to obtain mucilage/hydrogel (AVH) after cleaning from redundant materials manually and by sieving. The reagents and chemicals, that is, succinic anhydride, and *N,N*-dimethylacetamide (Alfa Aesar, Kandel Germany), 4-dimethylaminopyridine, NaOH, HCl, HNO_3, $NaHCO_3$, KBr, acetone, and n-hexane (Sigma-Aldrich, USA), $AgNO_3$, $NiCl_2{\cdot}6H_2O$, and $Co(NO_3)_2{\cdot}6H_2O$ (Riedel-de-Haen, Germany) used in the present study were of analytical grade (purity > 99%). Distilled water (reverse osmosis, RO) was used to perform batch experiments. All glassware was washed and rinsed first with distilled water and then with nitric acid (HNO_3) prior to use in experimental work.

2.2. Isolation of A. vulgaris seed mucilage

Pre-cleaned *A. vulgaris* seeds (AV) were immersed in distilled water (DW) for 24 h at room temperature (RT) prior to heat at 80°C for 30 min. The extruded mucilage (AVH) was detached by nylon mesh and then washed with DW. AVH was further de-fatted with *n*-hexane as per procedure described by Haseeb et al. [19]. Soon thereafter, AVH washed again with DW, centrifuged, and dried in an oven at 50°C under vacuum. The dried AVH was collected in an air-tight container after sieving through mesh sieve no. 60 and stored to use in experimental work. The yield of AVH (after vacuum drying and powdering) obtained as 13.0 g/100 g seeds.

2.3. Synthesis of acidic and sodic conjugates of AVH

AVH was esterified with succinic anhydride (SAn) synthesize its succinylated derivative, that is, SAV. Dimethylaminopyridine (DMAP) was used as catalyst. To do so, 3.0 g of AVH was immersed in 40 mL of N,N-dimethylacetamide (DMAc) and heated at 353 K under continuous stirring for 2 h. After that, succinic anhydride (SAn) (11.10 g) and DMAP catalyst (0.1 g) were added to the homogenized mixture of AVH and DMAc and kept under continuous stirring overnight at 353 K. The product thus obtained was cooled at RT and precipitated in 150 mL ethanol in replicate to avoid from unreactive SAn and bi-formation of succinic acid (SA). Formed esterified product, that is, SAV was collected, dried in an oven under vacuum at 50°C, sieved to make finely divided powder and stored in an air-tight jar at ambient temperature.

Yield: 82.7%; Degree of substitution (DS): 2.79/Anhydroglucose repeating unit of AVH.

Fourier transform infrared (FTIR) (KBr); 3,412 (OH; 2,936 (CH and CH_2; 1,740 ($C{=}O_{ester}$; and 1,035 (C–O–C) cm^{-1}.

For the synthesis of sodic conjugate of SAV, that is, Na-SAV, SAV was further agitated with a saturated aqueous solution of $NaHCO_3$ prepared by dissolving 16.0 g of

it in 200 mL DW for 2 h, at RT. The as-formed suspension was filtered to obtain Na-SAV and washed with DW till the removal of traces of $NaHCO_3$ and neutralization of filtrate. It was then air-dried and stored in an air-tight jar at ambient temperature to use as a sorbent for Ni(II) and Co(II) uptake from aqueous solution.

FTIR (KBr); 3,419 (OH); 2,927 (CH and CH_2); 1,740 ($C{=}O_{ester}$); 1,572 (COO^-); and 1,032 (C–O–C) cm^{-1}.

2.4. Determination of degree of substitution

Properties of any sorbent material depend manifestly on the degree of substitution value (DS). Therefore, to determine the DS value of acidic form of sorbent, that is, SAV, acidimetric titration method as described by Kohnke et al. [20] was employed with little manipulation in procedure. Briefly, 0.1 g of SAV was dispersed and stirred in aqueous solution of $NaHCO_3$ of known molarity (0.02 M) for 2 h. The filtrate of solution was taken to titrate against 0.02 M solution of HCl. The progress of titration was monitored using methyl orange indicator. Final volume of HCl obtained at the end of titration was noted and used to determine the DS value using following relations (Eqs. (1) and (2)):

$$n_{suc} = V_{NaHCO_3} \times M_{NaHCO_3} - V_{HCl} \times M_{HCl} \quad (1)$$

In above equation, n_{suc} denoted the total number of moles of carboxylic acid groups incorporated on to AVH, V_{NaHCO_3} is the volume of $NaHCO_3$ solution which was titrated against the net volume of V_{HCl} while M_{NaHCO_3} and M_{HCl} are the molarities of HCl and $NaHCO_3$, respectively.

$$DS = \frac{162.14 \times n_{suc}}{m_{SAV} - 100 \times n_{suc}} \quad (2)$$

where 162.14 embodies the molar mass (g mol^{-1}) of an anhydroglucose repeating unit of AVH (AGU) in for every succinate moiety, 100 is the increment added in the mass of an AGU in g mol^{-1} for each exchanged succinate group and m_{SAV} is the mass of SAV studied.

2.5. Calculation of yield

The efficiency of esterification reaction between AVH and SAn can be predicted by calculating theoretical yield. Given below relation (Eq. (3)) was embodies to determined it:

$$\text{Theoretical Yield} = m_{AVH} + \left[\frac{m_{SAV}}{M_{SAV}} \times DS \times M_{Suc} \right] \quad (3)$$

where, m_{AVH} is the mass of AVH used, m_{SAV} is the mass of succinylated AVH obtained, M_{SAV} is the molar mass of succinylated AVH obtained and was taken as per AGU, and M_{suc} denoted the molecular mass of succinate group.

2.6. Determination of sorbent point-zero charge pH

A pH at which surface of sorbent have no net charge due to equivalency in between the total positive and negative charges on sorbent surface is called as sorbent point-zero charge pH (i.e., pH_{ZPC}). One can easily deduce the chances of interaction between functional groups and metallic species of solution by knowing pH_{ZPC} of sorbent materials. Once the pH of solutions is greater than pH_{ZPC}, then the sorbent surface gets negative charge and attracts positively charged metallic species while if pH of said solutions is less than pH_{ZPC}, then sorbent surface gets positive charge and attracts negatively charged metallic species. Therefore, to judge the behavior of sorbents in connection to its capability for uptake of heavy metal ions and let the polluted water free from them, it is utmost important to analyze its pH_{ZPC}. For this purpose, pH-drift method as described by Khan and Sarwar [21] with little/necessary modification in protocol was used. Different solutions (100 mL each) were prepared in pH ranged from 2 to 10. This pH is referred as initial pH (pH_i). To adjust the pH_i of solutions, acidic (0.1 M HCl) or basic (0.1 M NaOH) solutions were utilized. Afterwards, 0.05 g sorbent Na-SAV was dispersed in the solutions and shaken in a rotary shaker for 2 h. The solutions were allowed to settle and final pH, that is, pH_f was determined to observe any fluctuation in pH. Plot of a graph between pH_f and pH_i, gives a line and a curve. The pH at which curve cross the line, that is, $pH_i = pH_f$, is taken as point-zero charge pH, that is, pH_{ZPC} of the sorbent Na-SAV [22].

2.7. FTIR Characterization and surface morphology of sorbent by scanning electron microscopy with energy-dispersive X-ray spectroscopy

FTIR (KBr) spectra of the sample (AVH) and products (SAV, Na-SAV, Co-SAV, and Ni-SAV) were acquired on the FTIR Prestige-21 spectrometer (Shimadzu, Japan). For this purpose, KBr pellet were prepared by mixing samples with KBr and then subjected to hydrolytic pressure for compression into a thin pellet form. Prepared pellets were allowed to dry at 50°C in an oven under vacuum for an hour and then spectrum were recorded in the wavenumber range 4,000–400 cm^{-1}. The surface morphology, topography, and structural diversity of AVH and SAV, Na-SAV (before and after uptakes of tested metals) were studied by capturing scanning electron microscopy (SEM)-images using SEM (Nova, NanoSEM 450) fitted with a low energy Everhart–Thornley detector (ETD) and by recording EDS spectrum using Oxford energy dispersive X-ray (EDX, Oxford). Samples were prepared by submerging dried materials (0.1 g) in DW. Moisture or air bubbling from samples was removed by sonication for half an hour. The sonicated samples were then freeze-dried and cross-sections (vertical and horizontal) were taken using sharp blades to assess its texture structure. Cross-sections of materials were further coated with gold with the help of a sputter coater (Denton, Desk V HP). Finally, SEM images and EDS spectrum were recorded.

2.8. Sorption experiments

Sorption studies were conducted to appraise the effect of various parameters, such as initial concentration, sorbent dose, pH, time of contact, and temperature on capacity of sorbent Na-SAV to adsorbed maximum amount of Ni(II)

and Co(II) from aqueous solution. For this purpose, standard solutions (1,000 mg g^{-1}, 1,000 mL) were prepared by the dissolution of fixed amounts of Ni(II) and Co(II) salts, that is, (4.05 g $NiCl_2 \cdot 6H_2O$) and (4.937 g $Co(NO_3)_2 \cdot 6H_2O$) in DW. The prepared standard solutions of both metals under investigation were further diluted as per requisite. 1.0 M solutions of HCl or NaOH was used adjust the pH of every running solution. An optimal quantity of sorbent Na-SAV, that is, 40 mg was added to 100 mg L^{-1} (100 mL) solution of each metal. The solution containing sorbent was then shaken using a shaking incubator for 30 min at RT. After that, the solutions were filtered to remove the sorbent and to get metal-based filtrate. The residual concentrations of Ni(II) and Co(II) in the obtained filtrate were estimated on FAAS at 232 and 240.7 nm wavelengths, respectively, for Ni(II) and Co(II). Sorption maxima (q_e in mg g^{-1}) and the % age removal efficiency of Na-SAV to remove Ni(II) and Co(II) were computed using the equations below [15]:

$$q_e = \frac{C_i - C_e}{m} \times V \tag{4}$$

$$\text{Percentage uptake} = \frac{C_i - C_e}{C_i} \times 100 \tag{5}$$

where q_e (mg g^{-1}) is the equilibrium sorption capacity, C_i (mg L^{-1}) is the initial concentration of Ni(II) and Co(II) in solutions, C_e (mg L^{-1}) is the residual concentration of Ni(II) and Co(II) in solutions, V (L) represents the volume of the solution used for sorption studies and m (g) is the mass of sorbent taken for sorption experiments.

2.8.1. Effect of initial concentration of metals

The influence of initial concentration of metal ions, that is, Ni(II) and Co(II) was studied to estimate the sorption maxima of the sorbent Na-SAV by feeding experimental sorption data to various isothermal models (Freundlich and Langmuir) and to optimize the ideal concentration metal ions. For this purpose, 40 mg sorbent (optimized) was stirred with 100 mL solution containing different concentrations of Ni(II) and Co(II), that is, 30, 50, 70, 90, 110, and 130 mg L^{-1} for 30 min at a speed of 200 rpm and RT.

2.8.2. Effect of sorbent dosage

To examine the minimum amount of sorbent Na-SAV at which maximum amount of Ni(II) and Co(II) removed from aqueous solution and sorption maxima achieved, different dosage of sorbent ranging from 20 to 100 mg were added to 50 and 70 mg L^{-1} solutions (optimized) having Ni(II) and Co(II), respectively. Each solution was stirred for 30 min at RT prior to analyze on FAAS.

2.8.3. Effect of pH

A pre-optimized amount of sorbent Na-SAV (40 mg) was added to 100 mL of 50 mg L^{-1} solutions of Ni(II) and 70 mg L^{-1} solutions of Co(II) at RT in order to monitor the dependency of sorption maxima on pH. Solutions of different pH (1–7) were prepared and run on FASS at prescribed wavelengths of tested metals.

2.8.4. Effect of contact time

The time of contact between sorbent and sorbate plays keen role to establish sorption kinetics. Therefore, it was studied. For this purpose, an optimum amount of sorbent (40 mg), at optimal initial metal ion concentration (50 mg L^{-1} for Ni(II) and 70 mg L^{-1} for Co(II)) and pH = 7, was dissolved in 100 mL solution containing Ni(II) and Co(II) at RT for different time intervals, that is, for 5–120 min. The sorption data obtained from this study was further put into linear forms of pseudo-first-, and pseudo-second-order kinetic equations and mechanism of sorption process was illustrated.

2.8.5. Effect of temperature

The influence of temperature on sorption process was also studied to know about the nature of sorption process. Temperature was varied from 298 to 343 K. Sorption experiments were run under pre-optimized conditions.

2.8.6. Sorption/desorption studies

Sorption/desorption studies were also conducted for this sorbent to check the effectiveness and reusability of it. To carry out these studies, sorbent Na-SAV were agitated with solution containing Ni(II) and Co(II) for 30 min at RT. As a result of this stirring sorbent might convert into Ni-SAV and Co-SAV. Soon thereafter, the solutions were filtered off and the recovered sorbents were treated with saturated aqueous solution of NaCl (brine, 100 mL) for desorption of Ni(II) and Co(II). The Ni(II) and Co(II) ions were substituted with Na^+ ions and sorbent Na-SAV was regenerated in both cases. This sorption/desorption process was repeated over five consecutive cycles for both Ni(II) and Co(II) and after each regeneration stage, the sorbent Na-SAV was centrifuged, air-dried and cleaned in DW till it showed no effect with $AgNO_3$. Acidic form of sorbent, that is, SAV was also utilized to conduct sorption experiments under similar conditions.

2.9. Determination of thermodynamic parameters

The experimental sorption data resulted from estimation of temperature effect on removal of metal ions from aqueous solutions was utilized to monitor the nature of sorption process and to also established sorption mechanism by computing various thermodynamic triplets, such as change in free energy ($\Delta G°$), enthalpy ($\Delta H°$), and entropy ($\Delta S°$) using the following equations [23]:

$$K_C = \frac{C_{\text{ads}}}{C_e} \tag{6}$$

$$\ln K_C = \frac{\Delta S°}{R} - \frac{\Delta H°}{RT} \tag{7}$$

$$\Delta G^\circ = -RT\ln K_C \quad (8)$$

where C_{ads} and C_e represents the quantity of metal sorbed and remaining concentration of Ni(II) and Co(II) mg g^{-1} at equilibrium, respectively. K_C is equilibrium constant for sorption process and R (8.314 JK^{-1} Mol^{-1}) is an ideal constant.

All the experimental work was performed in triplicate and average values along with standard deviation were interpreted.

3. Results and discussion

3.1. Synthesis of acidic and sodic conjugates of AVH

Being water insoluble, succinylated products and their conjugates can provide the basis for their utility as a potential sorbent to uptake ions of heavy metals from contaminated water. This sorption capability of sorbents may be interrelated to the existence of hydroxyl (–OH) and carboxylic acid (–COOH) moieties present in them which results in cross-linking of side chains [24]. Therefore, keeping in view the immense importance of succinylated products, acidic conjugate of AVH, that is, SAV was fabricated *via* esterification of AVH with SAn using DMAc as solvent. The as-obtained SAV was further converted to its sodic conjugate, that is, Na-SAV by tuning with saturated solution of $NaHCO_3$ (200 mL). The reaction yield was found to be 82.7%. The DS value of succinate moieties was determined on account of per AGU and achieved as 2.79.

3.2. FTIR spectroscopic characterization

The FTIR (KBr) spectra of AVH and products SAV, Na-SAV, Co-SAV, and Ni-SAV were recorded and incorporated in Fig. 1. Successful esterification of AVH was witnessed by the appearance of distinct and sharp carbonyl ester ($C{=}O_{ester}$) signals at 1,740 cm^{-1} in the FTIR spectrum of SAV and Na-SAV [25]. Furthermore, its saponification to sodic conjugate can be verified by a strong characteristics peak appeared at 1,572 cm^{-1} in the spectrum of Na-SAV due to carboxylate anion peak ($–COO^-$) [26]. Moreover, in the spectra of Co-SAV and Ni-SAV a slight shuffling in the intensity and position of peaks to lower wavenumber has also been observed due to formation of complex between carbonyl group and divalent Co(II) and Ni(II). Hence, witnessed the loading of both of these targeted metals onto sorbent Na-SAV [27,28].

3.3. Surface morphology of sorbent by SEM-EDS

The surface morphology of AVH, SAV, and Na-SAV (before and after the uptake of Ni(II) and Co(II)) and the presence of metal ions, that is, Na(I), Ni(II), and Co(II) in Na-SAV (before and after the uptake of Ni(II) and Co(II)) can be observed by SEM-EDS (Fig. 2a–i). The SEM-images of AVH (Fig. 2a), SAV (Fig. 2b), and Na-SAV (Fig. 2c) before and after Ni(II) and Co(II) uptake (Fig. 2d and e) indicate the bumpy, unsmooth and uneven surface morphology. EDS spectra of Na-SAV (before and after the uptake of Ni(II) and Co(II)) shows the presence of Na(I) (Fig. 2h), Ni(II) (Fig. 2i), and Co(II) (Fig. 2j), ions, respectively.

3.4. Determination of sorbent point-zero charge pH

The point-zero charge pH (pH_{ZPC}) of sorbent Na-SAV was found to be 4.75. This value indicated that the sorbent possesses weak acidic character and the exchange of Na^+ ions with Ni(II) and Co(II) might be facilitated (Fig. 3). Moreover, from pH_{ZPC} it can be illustrated that once the pH of solution is less than 4.75, then sorbent bear

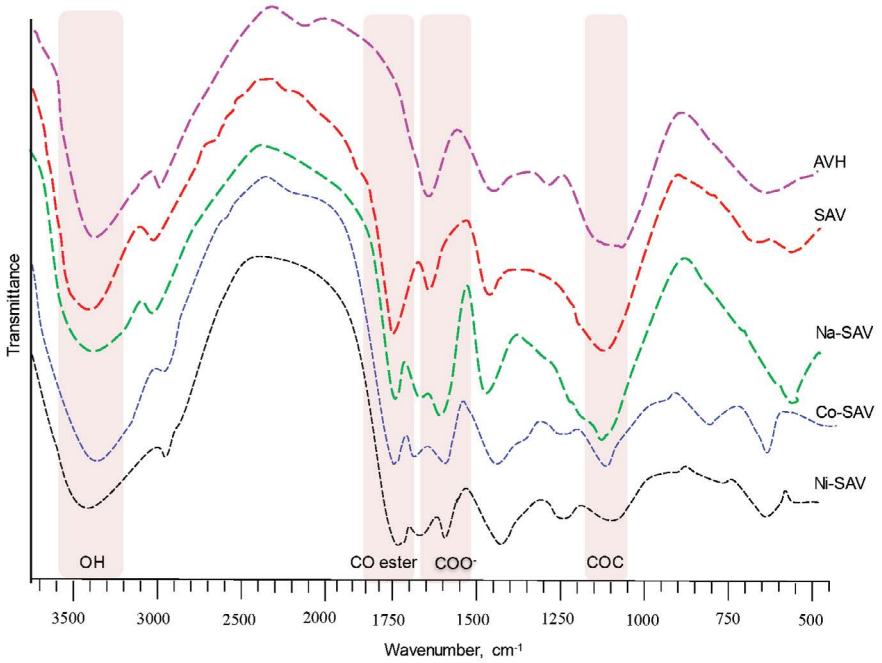

Fig.1. Overlay FTIR (KBr) spectrum of AVH, SAV, Na-SAV, Co-SAV, and Ni-SAV.

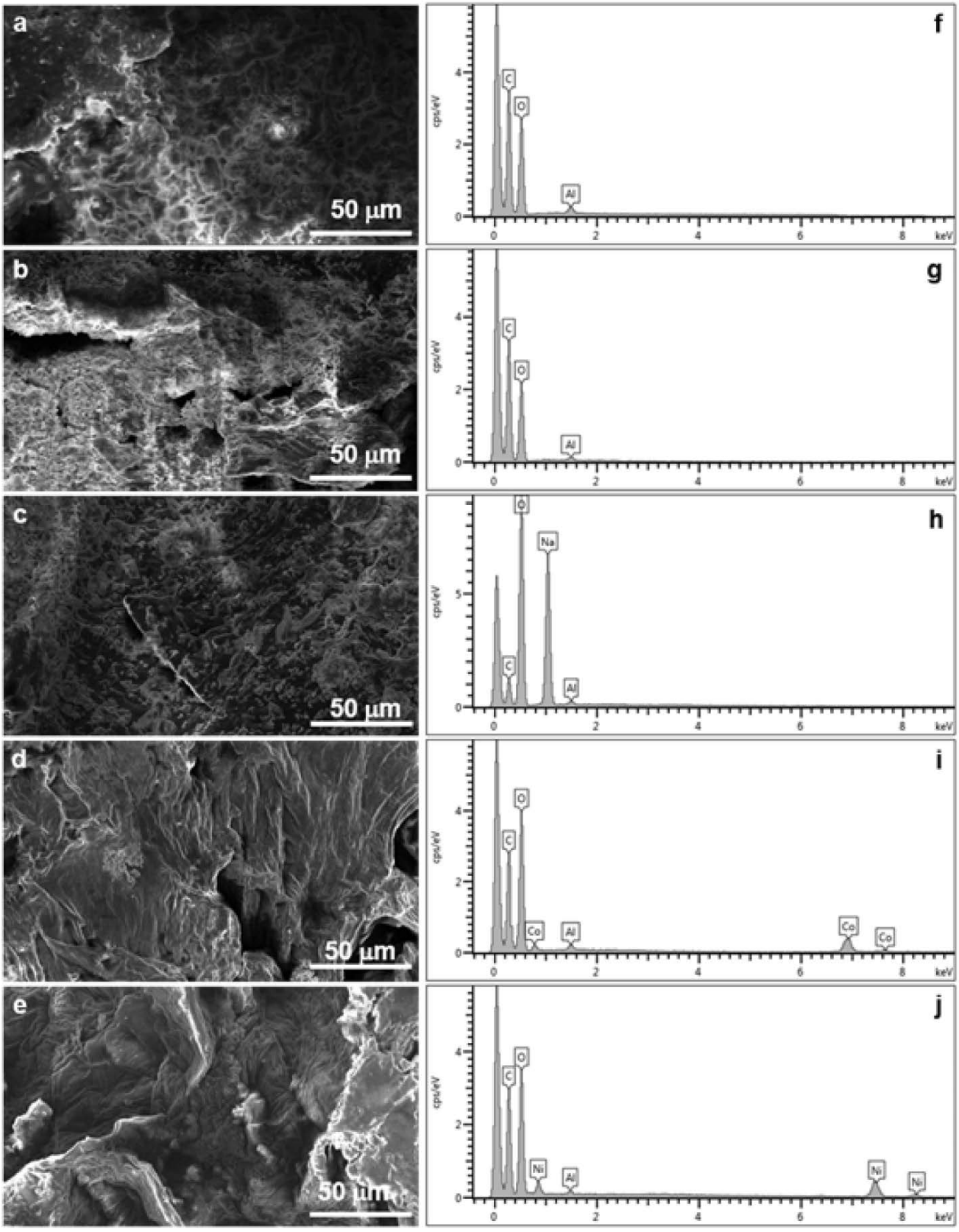

Fig. 2. SEM (a–e) and EDS (f–j) images of AVH (a and f), SAV (b and g), and Na-SAV (c–e and h–j). Panels (j and i) show the replacement of Na(I) by Co(II) and Ni(II).

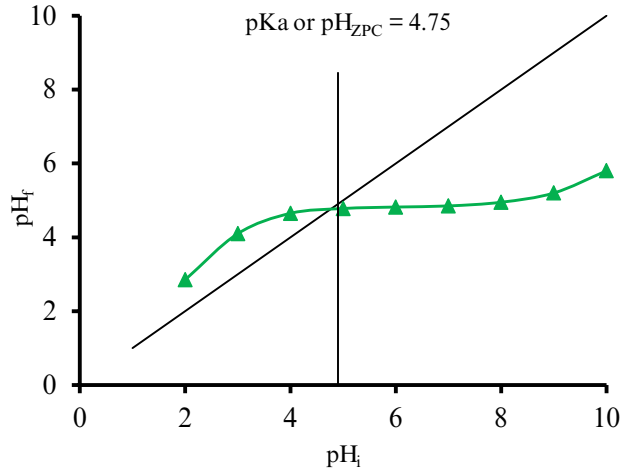

Fig. 3. Zero-point charge pH (pH_{ZPC}) analysis of Na-SAV.

positive charge on its surface and couldn't favor the sorption of heavy metal ions from polluted water whereas at pH greater than 4.75, the sorbent surface will have negative charge and favors the removal of Ni(II) and Co(II) from their prescribed aqueous solutions [16]. The zero-point charge pH (pH_{ZPC}) of the sorbent can also be explained on the basis of Henderson–Hasselbalch equation:

According to the Henderson–Hasselbalch equations.

$$\mathrm{pH} = \mathrm{pKa} + \log \frac{\left[\mathrm{AVH\ Succinate}^{-}\right]}{\left[\mathrm{AVH-COOH}\right]} \times 100 \tag{9}$$

Hence, when [AVH Succinate–] = [AVH–COOH], pKa = pH, which occurs when half of the weak acid groups of HA (here –COOH) are dissociated. Therefore, point of intersection in Fig. 3 can also be regarded as pKa value of the AVH succinate. Thus, when the initial pH is higher than pKa dissociation of COOH groups occurs and thus the pH is lowered. At pH > pKa, surface of the sorbent acquires negative charge which might facilitate the uptake of metal ions. When the initial pH < pKa, protonation occurs and the pH increases.

3.5. Sorption experiments

3.5.1. Effect of initial concentration of metals

The dependency of equilibrium sorption capacity (q_e in mg g^{-1}) on the concentration of Ni(II) and Co(II) in their prescribed aqueous solutions was evaluated to investigate the sorption pathways. It can be seen from Fig. 4a and b that the q_e of sorbent Na-SAV to sorbed ions of tested heavy metals increases as their concentration in aqueous solution increases and later it became persistent. The q_e reached to maximum value at 50 mg L^{-1} (118.3 mg g^{-1}) for Ni(II) and 70 mg L^{-1} (170.3 mg g^{-1}) for Co(II) which is because of the increase in availability of metal ions for sorbent Na-SAV at their higher concentration. However, after an optimum concentration, the sorbent surface became saturated due to exchange of metal ions [14]. Consequently, the q_e became constant.

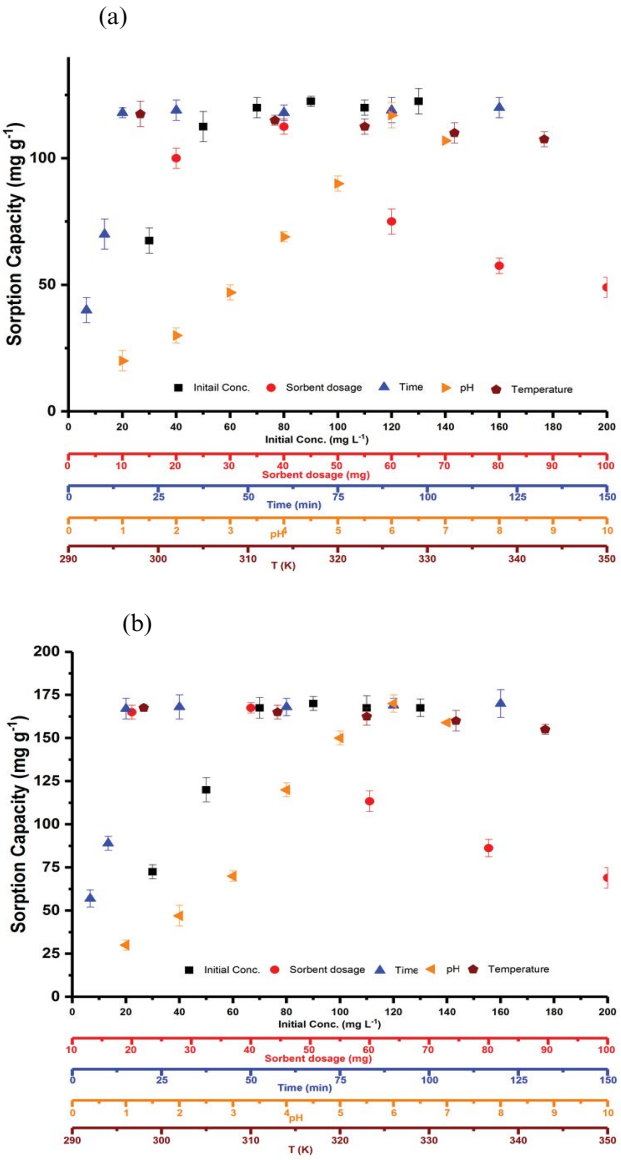

Fig. 4. Effect of initial concentration (black), sorbent dosage (red), pH (orange), time (blue), and temperature (wine) on sorption capacity of Na-SAV for removal of Ni(II) ions (a) and Co(II) ions (b).

3.5.2. Effect of sorbent dosage

Effect of sorbent dosage on equilibrium sorption capability of sorbent Na-SAV was studied to optimize its minimum dose at which sorption maxima achieved. It was revealed that with the increase in sorbent dosage, there was more uptake of Ni(II) and Co(II) but decreases significantly after achieving optimal quantity. This might be due to the reason that once the dose of sorbent is increases, it provided more and more active sites for sorption of heavy metal ions whereas no more ions were available to sorbed by the sorbent after optimum level. It is evidenced from the graph (Fig. 4a and b) that 40 mg of sorbent Na-SAV has maximum sorption capacity for the Ni(II) and Co(II) from their solutions.

3.5.3. Effect of pH

Effect of pH was studied to monitor the changes in sorbent surface charge (if any) and its degree of ionization during sorption process. The adsorbent sorbed a negligible amount of Co(II) and Ni(II) at acidic pH because the surface of sorbent containing carboxylate groups is now protonated and no free carboxylate groups are available to capture Co(II) and Ni(II) ions. However, the surface of the sorbent is negatively charged at a pH higher than 4.75 (pKa or pH_{ZPC}), due to dissociation of COOH groups which facilitates the uptake of Co(II) and Ni(II). The pH range selected for this investigation was 1.0–7.0 for both the heavy metals under study. Results of the experiment revealed that at low pH, the sorption of Ni(II) and Co(II) is negligible whereas with the increase in pH value the sorption capacity improved and reaches to maximum at pH 6 for both metals [29]. This low sorption capacity at low pH, that is, in acidic environment is might be due the fact that sorbent Na-SAV gets protonated and converted to acidic form of sorbent (SAV) which has worse ion-exchange ability while high sorption capacity at higher pH, that is, at pH > pKa or pH_{ZPC}, is might be due to the fact that sorbent gets deprotonated and its surface becomes negatively charged which favor the sorption of more and more positively charged metal ions [30,31]. From the graph (Fig. 4a and b), it can be witnessed that the ions of both heavy metals showed sorption maxima at a pH 6.

3.5.4. Effect of temperature

The investigation of effect of temperature on the ability of sorbent Na-SAV to sorbed metal ions helps to predict the nature of sorption mechanism. For this purpose, process of sorption was observed at various temperatures ranging from 298 to 343 K. Fig. 4a and b indicate that the sorption capacity decreases to some extent by increasing temperature. This decrease in sorption capacity confirmed the exothermic mode of sorption. The reason behind this trend might be that at low temperature, the mobility of Na^+ ions of sorbent is less and there is greater chance of the metal ions to get sorbed on the surface of sorbent Na-SAV. Contrary to this, when temperature is high, the Na(I) ions of sorbent becomes more mobile and chances of the metal ions to get sorbed on its surface becomes decrease. Hence, sorption capacity decreased. At 298 K sorption maxima was obtained both for the metal under study.

3.5.5. Effect of contact time

By knowing the time at which exchangeable sites of sorbent contact and exchangeable site of sorbate, we can better establish the sorption kinetics as well as sorption mechanism. For this purpose, sorption process was investigated by changing time from 5 to 120 min. Results as depicted in Fig. 4a and b show that about 85% of both Ni(II) and Co(II) get adsorbed on the surface of sorbent in the first 30 min from aqueous solution. This is due to the reason that at the beginning, large number of sodium succinate moieties might be present sorbent surface and the rate at which Ni(II) and Co(II) ions replaced with Na^+ ions is highest. Also from Fig. 4a and b, it can be seen that equilibrium was achieved after 30 min for both Ni(II) and Co(II) and no more significant increase in sorption was observed. Therefore, 30 min was selected as ideal time.

3.6. Isothermal modeling

Experimental sorption data resulted from the studies of effect of metal ion concentrations on equilibrium sorption capacity of sorbent Na-SAV was fitted to Freundlich and Langmuir isothermal models. This might help to study the relationship between actual concentration of sorbate in present in aqueous solution and its residual concentration under optimum conditions.

The Freundlich isotherm is usually applicable on heterogeneous systems and it can be used as a handicap tool to describe the nature of sorption process, that is, either monolayer or multilayer. The linear equation for the Freundlich isotherm is given in Eq. (10) [32]:

$$\log q_e = \log k_F + \frac{1}{n}\log C_e \tag{10}$$

where q_e (mg g^{-1}) is the concentration of metal ions sorbed per gram by Na-SAV, C_e (mg L^{-1}) is the concentration of heavy metal ions present at liquid level, constants involve in linear form of Freundlich equation, that is, k_F and n stands for sorption capacity and sorption strength, respectively. A graph was plotted by taking the values of $\log q_e$ along *Y*-axis and $\log C_e$ along *X*-axis. Straight lines as shown in Fig. 5 are obtained with slope, intercept and regression coefficient (R^2). Slope and intercepts of the straight lines gives the values of k_F and n. Also slope of the straight lines were used to calculate the sorption maxima (Q_{max} in mg g^{-1}) which were found to be highly deviated from experimental values (q_e in mg g^{-1}). Hence, the very low values of R^2 (<0.90) and the deviation of the values of Q_{max} from q_e showed that this model is not suitable to find the nature of sorption process for this study (Fig. 5 and Table 1). Therefore, the sorption data was further fitted to linear form Langmuir isothermal model as depicted in the following equation [33]:

$$\frac{C_e}{q_e} = \frac{C_e}{Q_{max}} + \frac{1}{Q_{max} \times b} \tag{11}$$

In Eq. (11), q_e and C_e have similar meaning as described earlier, while Q_{max} is the sorption maxima of sorbent Na-SAV in mg g^{-1} and b is the constant associated with linear form Langmuir isotherm. Plot of a graph between C_e/q_e vs. and C_e gives straight lines for both the heavy metals being tested with very high value of R^2 (>0.99). Slope of the straight lines give the values of Q_{max} and from intercept the values of b was calculated and tabulated. The values of Q_{max} (115.8 mg g^{-1} for Ni(II) and 170.7 mg g^{-1} for Co(II)) were found closest to the q_e (115.1 mg g^{-1} for Ni(II) and 170.0 mg g^{-1} for Co(II)) (Table 1). These evidences suggested that the sorbent under study, that is, Na-SAV has significantly greater number of sodium succinyl moieties which can also be evidenced from high DS value (2.79) of SAV. Hence, Langmuir model has been found to be ideally

to this sorption data which illustrated that the sorption followed chemisorption mechanism and occurred through a monolayer (Fig. 5). Furthermore, some essential features associated with Langmuir isotherm can also be explained by a dimensionless constant, that is, R_L (the separation factor). The value of R_L can be calculated for both Ni(II) and Co(II) using the following relation:

$$R_L = \frac{1}{1 + bC_i} \tag{12}$$

where C_i denoted the initial concentration of metal ions and determined in mg L^{-1} and b is an equilibrium constant which is associated with Langmuir isotherm and its dimension is L mg^{-1}. Sorption process is irreversible when $R_L = 0$, favorable for $0 < R_L < 1$, unfavorable for $R_L > 1$, and linear at $R_L = 1$. The value of R_L for both Ni(II) and Co(II) was found between 0 and 1 (Table 1) [34,35]. This might suggest favorable sorption.

Moreover, the difference in the values of sorption capacities, that is, 115.8 mg g^{-1} for Ni(II) and 170.7 mg g^{-1} for Co(II) can be described by the physical and chemical properties of the metal ions such as ionic radii, heat of hydration, electronegativity, softness capacity for hydroxylation, ionic potential, and position in the Irving–Williams series [36,37]. The first two factors namely ionic radii and heat of hydration plays an important role during their exchange in term of diffusion and site of exchange on the carboxylate adsorbent. The ionic radii of Co(II) and Ni(II) are 0.082 and 0.080 nm, respectively. Charge density (charge/ionic radius) of Ni(II) is greater than that of Co(II) because Ni(II) has lesser ionic radius while both have same charge (+2). Since charge density is directly related with heat of hydration thus Ni(II) has higher free energy of hydration (–494.2 kcal/g ion) while that of Co(II) is –479.5 kcal/g ion). Due to high value of heat of hydration, Ni(II) prefers to remain in solution phase. Thus, values of sorption capacities are in the order Co(II) > Ni(II). These values of ionic radii of Co(II) and Ni(II) also suggest that both of these ions can easily replace Na(I) with an ionic radius of 0.098 nm in the sorbent easily. Moreover, the interaction between sorbent and metal ion is purely electrostatic [36–38].

Moreover, Co(II) and Ni(II) were studied as single metal ion solution and no competitive sorption was studied.

3.7. Kinetic modeling

Pseudo-first- and pseudo-second-order kinetic model were used to fit the sorption data in order to elucidate the rate determining step and mechanism of sorption. Linear forms of pseudo-first- and pseudo-second-order kinetic models are depicted in Eqs. (13) and (14) [39, 40]:

$$\log\left(q_e - q_t\right) = \log q_e - \frac{k_1}{2.303}t \tag{13}$$

where q_e denotes the concentration of metal ions sorbed in mg g^{-1} on the surface of sorbent at equilibrium, q_t is the amount of metal sorbed in mg g^{-1} on the surface of sorbent at time t, k_1 is rate constant determined in g mg^{-1} $mint^{-1}$. Plot of graphs between $\log(q_e - q_t)$ and t gives straight lines very low value of R^2 for both metals. This low value of R^2 illustrated that pseudo-first-order kinetic model did not fit well to sorption data (Fig. 6 and Table 1).

The experimental sorption data obtained from contact time experiments was further subjected to linear form of pseudo-second-order kinetic model as depicted in Eq. (14):

$$\frac{t}{q_t} = \left(\frac{1}{kq_e^2} + \frac{t}{q_e}\right) \tag{14}$$

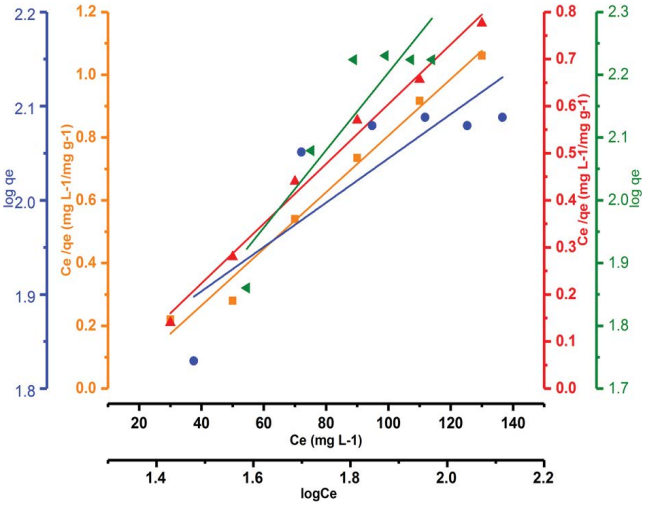

Fig. 5. Freundlich isotherm model (green for Co(II)) and (blue for Ni(II)) and Langmuir isotherm model for (red for Co(II)) and (orange for Ni(II)) metal uptake from aqueous solution by Na-SAV sorbent.

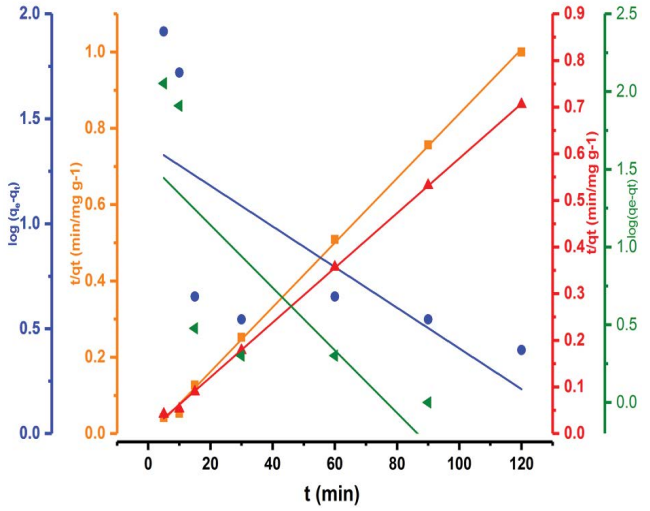

Fig. 6. Pseudo-first-order kinetic model (green for Co(II)) and (blue for Ni(II)) and pseudo-second-order kinetic model for (red for Co(II)) and (orange for Ni(II)) metal uptake from aqueous solution by Na-SAV sorbent.

Table 1
Pseudo-second-order, pseudo-first-order, Langmuir, Freundlich, ion-exchange models, and thermodynamic parameters for Ni(II) and Co(II) uptake by sorbent Na-SAV

Models	Parameters	Ni(II)	Co(II)
Pseudo-second-order	q_e (mg g^{-1})	118.3	170.3
	k_2 (g mg^{-1} min^{-1})	0.0098	0.0105
	R^2	0.9989	0.9995
Pseudo-first-order	q_e (mg g^{-1})	19.92	39.81
	k_1 (g mg^{-1} min^{-1})	0.022	–0.0461
	R^2	0.4751	0.5639
Experimental	q_e (mg g^{-1})	115.1	170
Langmuir parameters	Q_{max} (mg g^{-1})	115.8	170.7
	b (mg L^{-1})	0.0943	0.2127
	R^2	0.9849	0.9914
	R_L	0.1752	0.0632
Freundlich parameters	N	1.733	2.781
	k_F	11.74	22.75
	R^2	0.8325	0.7163
Ion exchange model	S (min^{-1})	–142.2	–66.66
	R^2	0.7496	0.9443
Thermodynamic parameters	$\Delta S°$ (J mol^{-1} K^{-1})	–0.2567	–1.333
	$\Delta H°$ (kJ mol^{-1})	–3.2143	–7.283
	R^2	0.96724	0.9678
	$\Delta G°$ (kJ mol^{-1})	–4.991	–6.432

where q_e (mg g^{-1}) and q_t (mg g^{-1}) represented the concentration of metal ions adsorbed on sorbent surface at equilibrium and time t, respectively, while k is the rate constant for pseudo-second-order kinetic model and it was determined in g mg^{-1} min^{-1}. A graph has been plotted between the values of t/qt against t to determine the kinetics of Ni(II) and Co(II) sorption. Straight lines with high values of R^2 (>0.99) were obtained which indicated the best fit of pseudo-second-order kinetic model to the experimental sorption data. Applicability of this kinetic model also suggested that the current sorption study involves chemisorption. Moreover, from the slope and intercepts of the straight lines the value of q_e (mg g^{-1}) and k was calculated and tabulated (Fig. 6 and Table 1).

3.8. Mechanism of sorption

The promising behavior of both SAV and Na-SAV to sorbed Ni(II) and Co(II) from aqueous solution was observed through the determination of mechanism involved during sorption process. Na-SAV showed very high uptake from both Ni(II) and Co(II), while SAV showed negligible sorption. The reason behind this deviation in sorption might be due to the exchange of ions, that is, exchange of Ni(II) and Co(II) ions of solutions with Na^+ ions of sorbent when dissolved in solution but due to unavailability of Na^+ ions in acidic form of sorbent (SAV) no such kind of exchange occur in between solutions containing Ni(II) and Co(II) and SAV. Ion-exchange mechanism involved in sorption could be explained by an equation given by Boyd [41]:

$$\log\left(1-F\right) = -\frac{S}{2.303}t \tag{15}$$

$$F = \frac{q_t}{q_e} \tag{16}$$

where q_e and q_t have same meaning as described before while S is a constant for sorption process which is measured in min^{-1}.

This equation was used to determine the rate of exchange of ions. The assumptions underlying this equation are as follows:

- This equation is applied to dilute solution of adsorbate, that is, Co(II) and Ni(II) solutions.
- There is a dynamic equilibrium between concentration of Co(II) and Ni(II) solutions in the adsorbent and concentration of adsorbate in the bulk.
- In order for distribution coefficient to be constant the adsorbate should be a micro-component of the system.
- Equilibrium at the surface of the adsorbing particle is assumed for all times of contact.

Plot between the values of log(1 – *F)* against t (Eq. (15)) gives straight lines with high value of R^2 for both Ni(II) and Co(II) which might predict that sorption process involved ion-exchange mechanism (Fig. 8a and Table 1). Fig. 7 illustrates the mechanism for ion-exchange of Co(II) and Ni(II) and their desorption in detail.

3.9. Determination of thermodynamic parameters

The feasibility, spontaneity, and nature of sorption process can be checked by calculating the values of certain thermodynamic parameters including $\Delta G°$, $\Delta S°$, and $\Delta H°$. The sorption data acquired from effect of temperature studies helps to determined said parameters. Plot of $\ln K_C$ vs. $1/T$ (K^{-1}) gives straight line (Fig. 8b). From the slope and intercepts, the value of $\Delta H°$ and $\Delta S°$ were determined and found to be negative. Later, these values were put into Eq. (8) to determine the value of $\Delta G°$ which is also found to be negative. The negative value of $\Delta S°$ is due to the presence of strong sorbent–sorbate interaction during the sorption process which might results decrease in the degree of freedom for sorbed Ni(II) and Co(II) on sorbent surface. Contrary to this, the negative values of $\Delta H°$ and $\Delta G°$ indicated the feasibility, spontaneity, and exothermic mode of sorption (Table 1).

3.10. Sorption/desorption studies

Experiments regarding sorption/desorption studies of Ni(II) and Co(II) were also carried out over five consecutive cycles and results are figured out. Co(II) and Ni(II) are studied as single metal ion solution and no competitive adsorption was studied. 15.0 and 17.0 mg g^{-1} decrease in sorption capacity was found for Ni(II) and Co(II), respectively after five repetitive cycles. Moreover, 11.5% and 10.5% decrease in percentage sorption was also

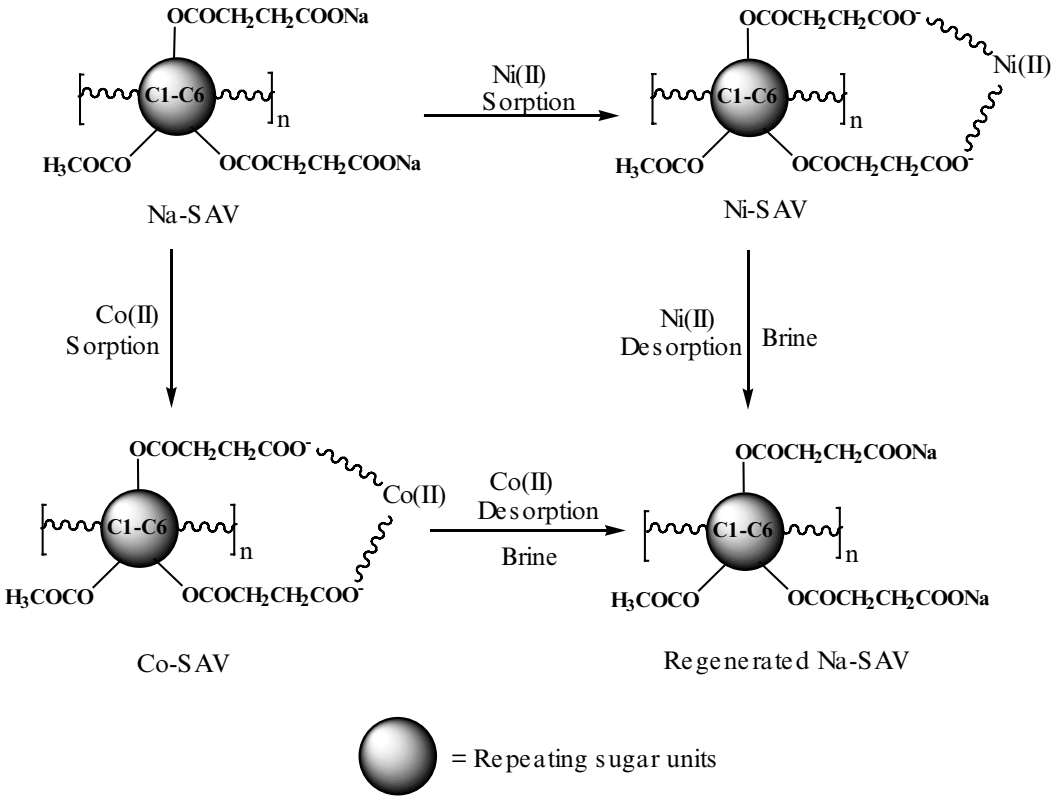

Fig. 7. Mechanism of adsorption and desorption of Ni(II) and Co(II) on the adsorbent.

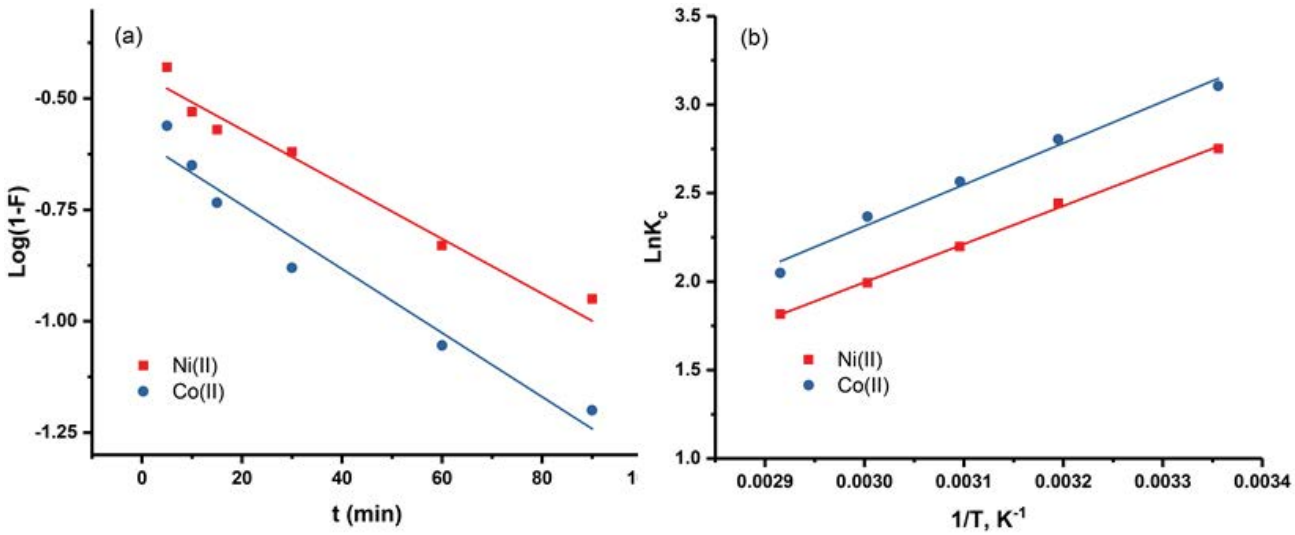

Fig. 8. Ion-exchange model (a) and effect of temperature on equilibrium constant (b) for Ni(II) and Co(II) sorption by Na-SAV.

found for Ni(II) and Co(II), respectively after five cycles (Fig. 9a and b). These results might infer that sorbent can be used repeatedly prior to replaced.

The comparison of position of the sorbent under study with other already reported modified and un-modified sorbents indicates that present sorbent has a distinct position among the other polysaccharidal sorbents for Ni(II) and Co(II) uptake as can be witnessed from Table 2.

The values of sorption capacities (Q_{max} in mg g^{-1}) of all the sorbent coated in Table 2 are calculated by Langmuir isothermal model.

4. Conclusions

A novel sodium salt of *A. vulgaris* hydrogel (Na-SAV) was conveniently synthesized by the succinylation of AVH

Table 2
Comparison of Na-SAV sorption capacity with other polysaccharide-based modified and un-modified reported sorbents for Ni(II) and Co(II) sorption

Sorbent	Target metal ion	Sorption capacity (mg g^{-1})	Ref.
Coir pith	Ni(II), Co(II)	15.95, 12.82	[42]
Brown seaweeds (*Sargassum wightii*)	Ni(II), Co(II)	18.58, 20.63	[43]
Gracilaria caudate and *Sargassum muticum*	Ni(II)	45, 70	[44]
Gum kondagogu	Ni(II)	50.5	[45]
Enteromorpha prolifera	Ni(II)	65.7	[46]
Chicken feathers (modified)	Ni(II), Co(II)	4.85, 50	[47]
Modified AVH	Ni(II), Co(II)	115.8, 170.7	Present study

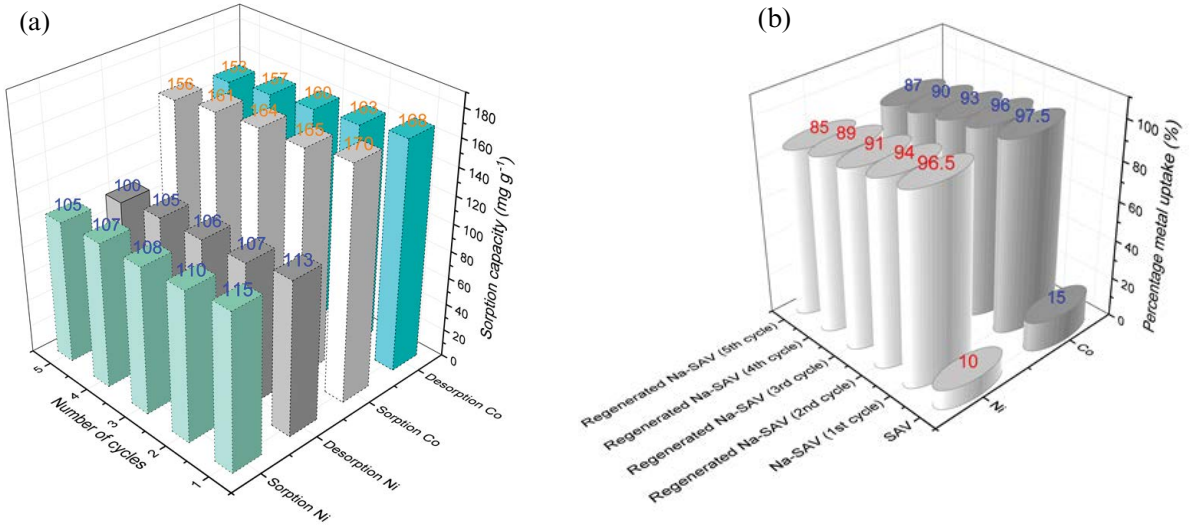

Fig. 9. Sorption/desorption studies for Ni(II) and Co(II) ions by the sorbent (Na-SAV) over five cycles from aqueous solutions by Na-SAV from aqueous solution (a) and percentage metal-uptake by the acidic (SAV) and sodic form of sorbent (Na-SAV) over five cycles from aqueous solutions by Na-SAV from aqueous solution (b).

followed by its treatment with $NaHCO_3$. The water insoluble sorbent appeared highly valuable for water purification by up taking toxic heavy metal ions. The Na-SAV appeared highly advantageous because of high sorption capacities (85%) for both Ni(II) and Co(II) from solution just within first 30 min of contact. Additional benefits noted for this benign sorbent Na-SAV are that it uptake the metal ion via rapid mechanism, that is, the ion-exchange *via* chemisorption as well as it showed high potential for re-usability. From thermodynamic data, it was inferred that sorption process was highly spontaneous and exothermic. Consequently, it can be stated that the sorbent Na-SAV is a supersorbent-biomaterial of great choice for industrial applications due to its commercial availability, economic nature, high sorption capacity, selectivity, efficient and spontaneous nature, re-usability, and ability to exchange ions.

Acknowledgments

We are grateful to ORIC University of Sargodha Pakistan for the financial support under grant number UOS/ORIC/2016/52 for the project "Removal of heavy metal ions from aqueous solution using chemically modified polysaccharide".

References

[1] Y. Xu, X. Dong, J. Miao, S. Wang, Z. Liu, Z. Zhai, L. Zhang, Z. Liu, Facile preparation of Ni, Co-alloys supported on porous carbon spheres for supercapacitors and hydrogen evolution reaction application, Int. J. Hydrogen Energy, 45 (2020) 1466–1476.
[2] B. Li, T. Mei, S. Du, W. Zhang, Synthesis of Ni-Fe and Ni-Fe/ZrO_2 composite coating and evaluation of its structural and corrosion resistance, Mater. Chem. Phys., 243 (2020) 122595, doi: 10.1016/j.matchemphys.2019.122595.
[3] H. Wu, X. Pang, J. Bi, L. Wang, Z. Li, L. Guo, H. Liu, Q. Meng, H. Jiang, C. Liu, L. Wang, Cellulose nanofiber assisted hydrothermal synthesis of Ni-rich cathode materials with high binding particles for lithium-ion batteries, J. Alloys Compd., 889 (2020) 154571, doi: 10.1016/j.jallcom.2020.154571.
[4] D. Kundu, T. Banerjee, Carboxymethyl cellulose-xylan hydrogel: synthesis, characterization, and *in vitro* release of vitamin B12, ACS Omega, 4 (2019) 4793–4803.
[5] Z. Wang, C. Yang, Metal carcinogen exposure induces cancer stem cell-like property through epigenetic reprograming: a

novel mechanism of metal carcinogenesis, Semin. Cancer Biol., 57 (2019) 95–104.
[6] B. Pesch, B. Kendzia, H. Pohlabeln, W. Ahrens, H.E. Wichmann, J. Siemiatycki, D. Taeger, W. Zschiesche, T. Behrens, K.H. Jockel, T. Bruning, Exposure to welding fumes, hexavalent chromium, or nickel and risk of lung cancer, Am. J. Epidemiol., 188 (2019) 1984–1993.
[7] L.O. Simonsen, H. Harbak, P. Bennekou, Cobalt metabolism and toxicology--a brief update, Sci. Total Environ., 432 (2012) 210–215.
[8] J. Wang, M. Liu, C. Duan, J. Sun, Y. Xu, Preparation and characterization of cellulose-based adsorbent and its application in heavy metal ions removal, Carbohydr. Polym., 206 (2019) 837–843.
[9] Y. Gossuin, A.L. Hantson, Q.L. Vuong, Low resolution bench top nuclear magnetic resonance for the follow-up of the removal of Cu^{2+} and Cr^{3+} from water by amber lite IR120 ion-exchange resin, J. Water Process Eng., 33 (2020) 101024, doi: 10.1016/j.jwpe.2019.101024.
[10] S. Fan, J. Zhou, Y. Zhang, Z. Feng, H. Hu, Z. Huang, Y. Qin, Preparation of sugarcane bagasse succinate/alginate porous gel beads via a self-assembly strategy: improving the structural stability and adsorption efficiency for heavy metal ions, Bioresour. Technol., 306 (2020) 123128, doi: 10.1016/j.biortech.2020.123128.
[11] Z. Zarghami, A. Akbari, A.M. Latifi, M.A. Amani, Design of a new integrated chitosan-PAMAM dendrimer biosorbent for heavy metals removing and study of its adsorption kinetics and thermodynamics, Bioresour. Technol., 205 (2016) 230–238.
[12] M.A. Hussain, G. Muhammad, I. Jantan, S.N.A. Bukhari, Psyllium arabinoxylan: a versatile biomaterial for potential medicinal and pharmaceutical applications, Polym. Rev., 56 (2016) 1–30.
[13] K.N. Awokoya, B.A. Moronkola, Preparation and characterization of succinylated starch as adsorbent for the removal of Pb(II) ions from aqueous media, Int. J. Eng. Sci., 1 (2012) 18–24.
[14] A. Abbas, M.A. Hussain, M. Sher, S.Z. Hussain, I. Hussain, Evaluation of chemically modified polysaccharide pullulan as an efficient and regenerable supersorbent for heavy metal ions uptake from single and multiple metal ion systems, Desal. Water Treat., 78 (2017) 241–252.
[15] B.A. Lodhi, A. Abbas, M.A. Hussain, S.Z. Hussain, M. Sher, I. Hussain, Design, characterization and appraisal of chemically modified polysaccharide based mucilage from *Ocimum basilicum* (basil) seeds for the removal of Cd(II) from spiked high-hardness ground water, J. Mol. Liq., 274 (2019) 15–24.
[16] G. Muhammad, A. Abbas, M.A. Hussain, M. Sher, S.N. Abbas, Chemically modified glucuronoxylan: a novel material for heavy metal ion removal from aqueous and spiked high hardness groundwater, Cellul. Chem. Technol., 52 (2018) 909–919.
[17] M.F.U. Haq, M.A. Hussain, M.T. Haseeb, M.U. Ashraf, S.Z. Hussain, T. Tabassum, I. Hussain, M. Sher, S.N.A. Bukhari, M.N.U. Hassan, A stimuli-responsive, superporous and non-toxic smart hydrogel from seeds of mugwort (*Artemisia vulgaris*): stimuli responsive swelling/deswelling, intelligent drug delivery and enhanced aceclofenac bioavailability, RSC Adv., 10 (2020) 19832–19843.
[18] M.F.U. Haq, A. Ali, M.A. Hussain, A. Abbas, F. Kausar, H.M.A. Amin, M. Sher, S.Z. Hussain, I. Hussain, chemical modification of a polysaccharide from *Artemisia vulgaris* engenders a supersorbent for the removal of Cd^{2+} from spiked high-hardness groundwater, Desal. Water Treat., 212 (2021) 129–142.
[19] M.T. Haseeb, M.A. Hussain, S.H. Yuk, S. Bashir, M. Nauman, Polysaccharides based superabsorbent hydrogel from Linseed: dynamic swelling, stimuli responsive on-off switching and drug release, Carbohydr. Polym., 136 (2016) 750–756.
[20] T. Kohnke, A. Ostlund, H. Brelid, Adsorption of arabinoxylan on cellulosic surfaces: influence of degree of substitution and substitution pattern on adsorption characteristics, Biomacromolecules, 12 (2011) 2633–2641.
[21] K.N. Khan, A. Sarwar, Determination of points of zero charge of natural and treated adsorbents, Surf. Rev. Lett., 14 (2007) 461–469.
[22] A. Abbas, M.A. Hussain, M. Sher, M.N.U. Hassan, Chemically modified hydroxyethylcellulose: a high capacity sorbent for removal of As(III) and As(V) from aqueous solution, Desal. Water Treat., 104 (2018) 149–158.
[23] E.C. Lima, A.H. Bandegharaei, J.C.M. Piraján, I. Anastopoulos, A critical review of the estimation of the thermodynamic parameters on adsorption equilibria. Wrong use of equilibrium constant in the Van't Hoof equation for calculation of thermodynamic parameters of adsorption, J. Mol. Liq., 273 (2019) 425–434.
[24] A. Abbas, M.A. Hussain, M. Sher, M.I. Irfan, M.N. Tahir, W. Tremel, S.Z. Hussain, I. Hussain, Design, characterization and evaluation of hydroxyethylcellulose based novel regenerable supersorbent for heavy metal ions uptake and competitive adsorption, Int. J. Biol. Macromol., 102 (2017) 170–180.
[25] S.N. Abbas, M. Amin, M.A. Hussain, K.J. Edgar, M.N. Tahir, W. Tremel, Extended release and enhanced bioavailability of moxifloxacin conjugated with hydrophilic cellulose ethers, Carbohydr. Polym., 136 (2016) 1297–1306.
[26] M.A. Hussain, S. Zaman, A. Abbas, M.N. Tahir, M. Amin, S.Z. Hussain, I. Hussain, Sodium hyroxyethylcellulose adipate: an efficient and reusable sorbent for cadmium uptake from spiked high-hardness ground water, Arabian J. Chem., 13 (2020) 2766–2777.
[27] E. Fourest, B. Volesky, Contribution of sulfonate groups and alginate to heavy metal biosorption by the dry biomass of *Sargassum fluitans*, Environ. Sci. Technol., 30 (1996) 277–282.
[28] L. Fuks, D. Filipiuk, M. Majdan, Transition metal complexes with alginate biosorbent, J. Mol. Struct., 792–793 (2006) 104–109.
[29] H. Wang, Z. Wang, R. Yue, F. Gao, R. Ren, J. Wei, X. Wang, Z. Kong, Functional group-rich hyper branched magnetic material for simultaneous efficient removal of heavy metal ions from aqueous solution, J. Hazard. Mater., 384 (2020) 121288, doi: 10.1016/j.jhazmat.2019.121288.
[30] S. Bao, W. Yang, Y. Wang, Y. Yu, Y. Sun, One-pot synthesis of magnetic graphene oxide composites as an efficient and recoverable adsorbent for Cd(II) and Pb(II) removal from aqueous solution, J. Hazard. Mater., 381 (2020) 120914, doi: 10.1016/j.jhazmat.2019.120914.
[31] K. Tizaoui, B. Benguella, B. Makhoukhi, Selective adsorption of heavy metals (Co^{2+}, Ni^{2+}, and Cr^{3+}) from aqueous solutions onto natural marne clay, Desal. Water Treat., 142 (2019) 252–259.
[32] H.M.F. Freundlich, Over the adsorption in solution, Z. Phys. Chem., 57 (1906) 385–470.
[33] I. Langmuir, The constitutional and fundamental properties of solids and liquids, J. Am. Chem. Soc., 38 (1916) 2221–2295.
[34] S. Bahah, S. Nacef, D. Chebli, A. Bouguettoucha, B. Djellouli, A new highly efficient Algerian clay for the removal of heavy metals of Cu(II) and Pb(II) from aqueous solutions: characterization, fractal, kinetics, and isotherm analysis, Arabian J. Sci. Eng., 45 (2020) 205–218.
[35] F. Boudrahem, F.A. Benissad, A. Soualah, Kinetic and equilibrium study of the sorption of lead(II) ions from aqueous phase by activated carbon, Arabian J. Sci. Eng., 38 (2013) 1939–1949.
[36] D. Ouyang, Y. Zhuo, L. Hu, Q. Zeng, Y. Hu, Z. He, Research on the adsorption behavior of heavy metal ions by porous material prepared with silicate tailings, Minerals, 9 (2019) 1–16.
[37] A. Manel, E. Elimame, The removal of cadmium, cobalt, and nickel by adsorption with Na-Y Zeolite, Iran. J. Chem. Chem. Eng., 39 (202) 169–179.
[38] H. Mekatel, S. Amokrane, A. Benturki, D. Niboua, Treatment of polluted aqueous solutions by Ni^{2+}, Pb^{2+}, Zn^{2+}, Cr^{6+}, Cd^{+2} and Co^{+2} ions by ion exchange process using faujasite zeolite, Procedia Eng., 33 (2012) 52–57.
[39] S. Lagergren, B.K. Svenska, On the theory of so-called adsorption of materials, R. Swed. Acad. Sci. Doc Band, 24 (1898) 1–13.
[40] Y.S. Ho, G. McKay, Pseudo-second-order-model for sorption processes, Proc. Biochem., 34 (1999) 451–465.
[41] G.E. Boyd, A.W. Adamson, L.S. Myers, The exchange adsorption of ions from aqueous solutions by organic zeolites. II. Kinetics, J. Am. Chem. Soc., 69 (1947) 2836–2848.

[42] H. Parab, S. Joshi, N. Shenoy, A. Lali, U.S. Sarma, M. Sudersanan, Determination of kinetic and equilibrium parameters of the batch adsorption of Co(II), Cr(III) and Ni(II) onto coir pith, Process Biochem., 41 (2006) 609–615.
[43] K. Vijayaraghavan, J. Jegan, K. Palanivelu, M. Velan, Biosorption of cobalt(II) and nickel(II) by seaweeds: batch and column studies, Sep. Purif. Technol., 44 (2005) 53–59.
[44] Y.G. Bermudez, I.L.R. Rico, O.G. Bermudez, E. Guibal, Nickel biosorption using *Gracilaria caudata* and *Sargassum muticum*, Chem. Eng. J., 166 (2011) 122–131.
[45] V.T. Vinod, R.B. Sashidhar, B. Sreedhar, Biosorption of nickel and total chromium from aqueous solution by gum kondagogu (*Cochlospermum gossypium*): a carbohydrate biopolymer, J. Hazard. Mater., 178 (2010) 851–860.
[46] A. Ozer, G. Gurbuz, A. Calimli, B.K. Korbahti, Investigation of nickel(II) biosorption on *Enteromorpha prolifera*: optimization using response surface analysis, J. Hazard. Mater., 152 (2008) 778–788.
[47] R. Chakraborty, A. Asthana, A.K. Singh, S. Yadav, M.A.B.H. Susan, S.A.C. Carabineiro, Intensified elimination of aqueous heavy metal ions using chicken feathers chemically modified by a batch method, J. Mol. Liq., 312 (2020) 113475, doi: 10.1016/j.molliq.2020.113475.